Phys. Rev. 174, 392 (1968).
[18]E. Uggerhøj, Phys. Letters 22, 382 (1966).
[19]R. Behnish, F. Bell, and R. Sizmann, Phys. Status Solidi 33, 375 (1969).
[20]P. N. Tomlinson and A. Howie, Phys. Letters 27A, 491 (1968).

PHYSICAL REVIEW B VOLUME 2, NUMBER 7 1 OCTOBER 1970

Optical Properties of Divalent Manganese in Calcium Fluorophosphate

F. M. Ryan, R. C. Ohlmann, J. Murphy,
R. Mazelsky, G. R. Wagner, and R. W. Warren
Westinghouse Research Laboratories, Pittsburgh, Pennsylvania 15235
(Received 30 April 1970)

We have studied the optical absorption, fluorescence excitation, and fluorescence emission spectra of single crystals of calcium fluorophosphate containing divalent manganese. A comparison of these measurements with electron-spin-resonance measurements made on the same crystals has enabled us to identify the optical excitation and emission spectra of divalent-manganese ions located on each of three inequivalent sites in the lattice. The sites observed are the Ca(I)-type site, the Ca(II)-type site, and a site similar to the Ca(II) site except with a "modified" environment. A fourth site, a "modified" Ca(I)-type, has been detected by electron spin resonance, but its optical properties could not be obtained. The excitation and emission spectra of manganese on the Ca(I), Ca(II), and Ca(II) "modified" sites are presented, as well as a discussion of the effects of temperature, manganese concentration, and crystal-growth conditions on the optical properties of the crystals.

I. INTRODUCTION

The calcium fluorophosphate or fluorapatite system (FAP) doped with manganese has been the object of considerable interest over the last two decades, primarily because of the commercial value of fluorescent-lamp phosphors using the halophosphate system. Fluorapatite has the hexagonal space group $P6_3/m$ (C_{6h}^2) with two molecules of $Ca_5(PO_4)_3F$ per unit cell. There are two inequivalent sites for the Ca^{+2} ions in this structure, 40% of the Ca^{+2} ions being on the so-called Ca(I) sites with the remainder on the Ca(II) sites. The Ca(I) site has C_3 point-group symmetry with each calcium ion having six oxygen nearest neighbors which form a slightly twisted triangular prism about it. The Ca(II) site has C_{1h} point-group symmetry with the Ca^{+2} ions sitting at the corners of equilateral triangles with an F^- ion in the center. Mn^{+2} ions are expected to enter FAP crystals by simple substitution for Ca^{+2} ions on either the Ca(I) or the Ca(II) sites. However, if one includes the possibility of interstitial sites, interactions with other crystalline imperfections, and manganese valence states higher than +2, the number of ways in which manganese could be incorporated into a FAP crystal becomes quite large. Although optical and ESR measurements have been made on halophosphate powders by others, [1-3] the complexity of the apatite crystal structure is such that limited progress was made in deciding between these alternatives until single crystals of FAP become available. Johnson[2] was the first to successfully grow crystals of FAP using the Czochralski method. He doped some of his crystals with manganese and measured their optical properties and attempted to deduce the site(s) of the manganese ions. [2,4,5] We find that the optical emission that Johnson observed and ascribed to Mn^{+2} is very strong in most crystals but is due not to Mn, but instead to a defect center associated with the deviation of the crystals from stoichiometry. We have studied the optical properties of this defect center (termed here the "*X*" center) and how its concentration can be altered both by variations in the stoichiometry of the melt and by the addition of manganese to it. We have been able to study the true optical properties of manganese in FAP only after separating out the optical properties of this defect center. When the optical properties of manganese are correlated with ESR measurements, we are able to divide the excitation and emission spectra of manganese into three or more parts due to manganese in three or more sites. A discussion of the description of these sites and the optical properties of manganese at each site is the purpose of this paper.

II. CRYSTALS

The fluorapatite crystals were grown by the Czochralski technique using induction heating. The equipment and techniques used have been described previously. [6] An iridium crucible served as both container and susceptor and is the most satisfactory container material found since it is neither wet nor

attacked by molten fluorapatite. All chemicals used as starting materials were of luminescent grade. The starting charge and the reaction by which it is converted to fluorapatite upon heating are represented by the formula

$$CaF_2 + 6CaHPO_4 + (3-x)CaCO_3 + xMnCO_3$$

$$\rightarrow Ca_{(10-x)}Mn_x(PO_4)_6F_2 + 3H_2O + (3)CO_2.$$

Crystals pulled from this stoichiometric composition are found to be deficient in calcium fluoride.[7] To grow crystals with the stoichiometric composition, we have used melts containing large excesses of CaF_2. However, if the growth is too rapid, inclusions of CaF_2 are visible in the crystal. With slow growth the excess CaF_2 has sufficient time to diffuse away from the solid-liquid interface of the growing crystal. A series of crystals were grown from melts containing 3 parts of $Ca_3(PO_4)_2$ + (0.6, 0.7, 0.9, 1.2, 1.5, 1.8, 2.1, 2.5, and 3) parts of CaF_2. These represent a large variation from fluoride-deficient to fluoride-excess melts. The composition $3Ca_3(PO_4)_2 + 1.0\ CaF_2$ corresponds to a stoichiometric melt. These crystals are discussed in the part of this paper dealing with X centers (Sec. V).

The manganese-doped crystals grown for this work are listed in Table I. They consist of crystals doped with various concentrations of manganese pulled from both stoichiometric melts and melts off stoichiometry. The concentration of manganese in the crystals determined by ESR are included in Table I.

Because the Mn^{+2} ion is 20% smaller than the Ca^{+2} ion, one would expect to find a considerable deviation from unity of the segregation coefficient of Mn. Chemical and x-ray fluoresence determination as well as ESR measurements of manganese in the crystal have been made and indicate a segregation coefficient between 0.1–0.3 over the range of Mn concentrations studied.

III. OPTICAL MEASUREMENTS

Optical measurements were performed at 300 77, 4.2, and 1.8 °K. At 1.8 °K the crystals were directly immersed in liquid helium below the λ point to eliminate bubbling. In most cases the absorption by Mn was very low so that only excitation and fluorescence measurements were made. A 500-W Hanovia xenon arc and two tandem $\frac{1}{4}$-m Jarrell-Ash grating spectrometers were used for excitation. The fluorescence was detected by either an S-1 or an S-20 photomultiplier after passing through either a $\frac{1}{4}$-m Jarrell-Ash grating spectrometer or suitable combinations of interference and Corning filters, depending on the energy and wavelength of the fluorescence. The entire system was corrected to obtain an energy response for both polarizations of both excitation and fluorescent spectra.

In the course of our measurements, we encountered difficulties in attempting to measure the excitation spectra of crystals with very dilute manganese concentrations because the manganese fluorescence was masked by spurious fluorescence (such as from the X center) and false light from the excitation monochromator. This difficulty was avoided by installing a 71-cps square-wave chopper between the xenon light source and the excitation monochromator to alternately pass the excitation light for 7 msec and then block it for 7 msec, and by detecting the fluorescence from the crystal with specially constructed S-1 and S-20 grid-controlled photomultipliers[8] gated to detect light only during the middle 6 msec of the 7-msec "off" period. This combination will detect light only if it is delayed 1 msec or more. The decay time of manganese in FAP is 8 msec compared to about 1 μsec for the X-center luminescence and about 100 μsec for the source light. Thus, the chopper and gated photomultiplier enabled us to achieve a high degree of rejection of false light and luminescence (a ratio of over 100:1 was actually achieved). A block diagram of this system is shown in Fig. 1.

TABLE I. List of crystals, melt compositions, and ESR determinations of site occupancies.

Crystal designation	$\frac{Mn}{Ca}$ in melt	$\frac{Mn}{Ca}$ in Ca(I) site	$\frac{Mn(II)}{Mn(I)}$	$\frac{Mn(II\,m)}{Mn(I)}$	$\frac{Mn(I\,m)}{Mn(I)}$	CaF_2 in melt	$\frac{\sum Mn}{Mn(I)}$
0.1% Mn	1.0×10^{-3}	6.8×10^{-5}	0.08	2.3	0.07	Stoch.	3.4
1% Mn	1.0×10^{-2}	4.9×10^{-4}	0.2	1.5	0.09	Stoch.	2.7
3% Mn	3.0×10^{-2}	3.0×10^{-3}	0.5	0.4	0.02	Stoch.	2.1
10% Mn	1.0×10^{-1}	1.0×10^{-2}	(0.67	other	Mn)	Stoch.	1.7
0.1% Mn, $3\times CaF_2$	1.0×10^{-3}	1.3×10^{-4}	0.10	0.09	0.16	$3\times$Stoch.	1.4
1% Mn, $3\times CaF_2$	1.0×10^{-2}	1.0×10^{-3}	0.14	0.10	0.11	$3\times$Stoch.	1.4
3% Mn, $3\times CaF_2$	3.0×10^{-2}	6.2×10^{-3}	0.31	0.11	0.10	$3\times$Stoch.	1.4
10% Mn, $3\times CaF_2$	1.0×10^{-1}	2.2×10^{-2}	(0.63	other	Mn)	$3\times$Stoch.	1.6
0.1% Mn, CaO def	1.0×10^{-3}	5.3×10^{-4}	0.18	0	0	Stoch.	1.2

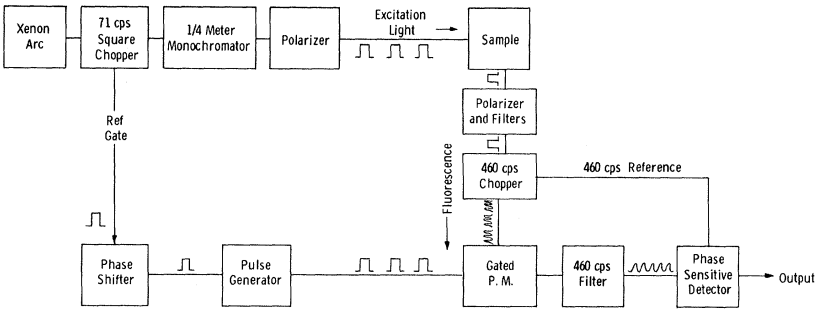

FIG. 1. Diagram of excitation arrangement.

The decay times of Mn and the X center and a time-resolved emission spectra of each were measured using a PAR waveform eductor and integrating gate. The time-resolved measurements were made using 1-μsec-long pulses of 15-kV electrons to excite the crystals because of the improved stability possible using this technique over flash-lamp excitation. The decay measurements were performed using both xenon flash lamps and electron-beam excitation at very low current densities to eliminate errors due to bimolecular quenching of the manganese fluorescence.[9]

IV. ELECTRON SPIN RESONANCE

The crystals were analyzed for Mn by ESR spectroscopy. The spectra show four sets of strong lines due to Mn^{2+} in four different environments. They are called Mn(I), Mn(II), Mn(Im), and Mn(IIm) lines to imply that the corresponding Mn ions are in the Ca(I), Ca(II), and "modified" Ca(I) and Ca(II) sites. This identification is accomplished in part by information which can be extracted from the ESR spectra about the symmetry of each site, i.e., that the Mn(I) center has axial symmetry, the Mn(II) center-reflection symmetry in the c plane, and the Mn(Im) and Mn(IIm) centers no symmetry. These conditions are exclusive enough to make the identifications of Mn(I) and Mn(II) sites as normal Ca(I) and Ca(II) sites very likely but are little help in confirming our models for the Mn(Im) or Mn(IIm) sites. To do this we have relied upon other, more indirect, evidence, and arguments such as the following: (a) We can alter the concentrations of Mn(Im) and Mn(IIm) centers by growing crystals from a melt with a nonstoichiometric concentration of CaO or CaF_2. This suggests that the Mn(Im) and Mn(IIm) centers include additional defects of some kind whose concentrations are sensitive to these variations – most likely oxygen and/or vacancy defects substituted for F^- ions. (b) We have found evidence for the existence of a strong attraction between Mn ions and oxygen-vacancy defects. This attraction is likely to lead to the closest possible spacings between them, i.e., Mn at a Ca(II) position and an oxygen-vacancy defect at the nearby fluorine sites. We identify this complex with the most common modified site Mn(IIm). (c) The Mn ions at Ca(I) sites might also be expected to form bonds with oxygen-vacancy defects but, due to the necessarily larger spacing between them, the bonds would be weaker and the ESR spectra of this center would be closer to that of the Mn(I) center than the Mn(IIm) is to the Mn(II) center. The Mn(Im) spectra satisfy these expectations, so that we identify them with this complex.

Kasai[3] has previously observed and identified the Mn(I) ESR spectrum in powders and Ohkubo and others[10] in single crystals. Ohkubo and Mizuno[11] have observed a spectrum similar to Mn(II) in chloroapatite crystals and have identified it as we have. No spectra similar to Mn(Im) or Mn(IIm) have been reported. Details concerning these centers will be found in an article to be published.

Table I indicates the concentrations of the Mn(I), Mn(II), Mn(Im), and Mn(IIm) centers in several crystals grown from melts containing various Mn concentrations and different amounts of CaF_2 or, in one case, CaO. "St" indicates the melt had the apatite composition. "3×CaF_2" means that the CaF_2 concentration was three times higher. "CaO def" means that the CaO concentration was 10% lower. The Mn concentrations were determined from measurements of the relative areas of their ESR spectra and from a chemical determination of the total Mn content of one sample. The resonance lines in the spectra broaden as the Mn concentration is increased. In the samples with most Mn, the Mn(II), Mn(Im), and Mn(IIm) contributions could not be distinguished from each other, therefore, only their sum is reported as "other Mn." The accuracy of the measurements is about ± 25%.

The conclusions drawn from Table I which are useful in interpreting the composite Mn excitation and emission envelopes can be summarized in the following manner:

(1) $\frac{\text{Mn(I}m\text{)}}{\text{Mn(I)}} \cong 0.1$ independent of manganese concentration for stoichiometric

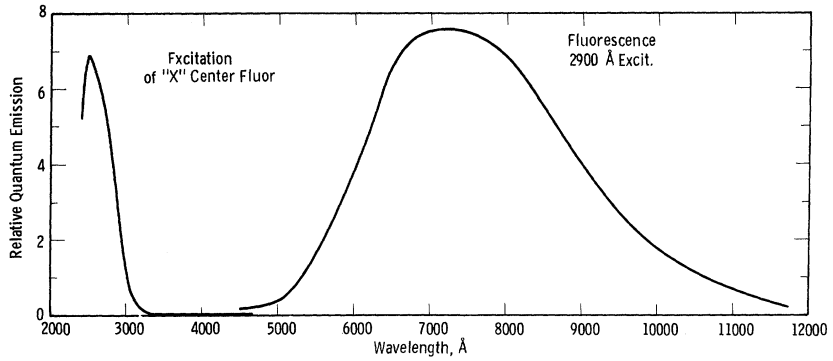

FIG. 2. Excitation and fluorescence emission spectra of the X center.

melts or melts containing excess CaF_2,

$\cong 0$ for CaO-deficient melts;

(2) $\frac{Mn(II_m)}{Mn(I)}$ $\cong 0.1$ independent of manganese concentration for melts containing excess CaF_2,

$\cong 0.0$ for CaO-deficient melts,

> 2 for low manganese concentrations in stoichiometric melts, dropping to less than 0.4 for melt concentrations over 3%;

(3) $\frac{Mn(II)}{Mn(I)}$ < 0.1 for low manganese concentrations increasing to more than 0.6 for melt concentrations of 10%, independent of growth conditions.

V. OPTICAL PROPERTIES OF X CENTER

Figure 2 shows the fluorescence and excitation spectra that Johnson believed was due to manganese +2. We find it present in crystals containing no Mn and have labeled the unidentified center responsible the "X" center. It is probably the same as the center termed "O_x" by Prener, Piper, and Chrenko[12] and identified by them as an unknown configuration of fluorine-ion vacancies and substitutional oxygen. Its fluorescence is 100% polarized with its electric vector parallel to the c axis of the crystals (π). It is the only luminescence center we have seen in FAP that is so strongly polarized. It is orange in color at 300 °K, changing to red at low temperatures as its emission envelope shifts to longer wavelengths. The X-center decay time is about 1 μsec. Its excitation spectrum is also strongly polarized parallel to the c axis. The corresponding absorption is similarly polarized and is very strong. The excitation spectrum shifts to higher energies at lower temperatures. This shift amounts to about 200 Å between 2 and 300 °K.

Crystals free of X-center fluorescence have been prepared in at least three ways: (a) by adding a large excess of CaF_2 to a stoichiometric melt. Undoped crystals pulled from a wide range of off-stoichiometric melts showed a monatonic decrease in the intensity of X-center fluorescence as the amount of CaF_2 in the melt was increased. Chemical analyses performed on these crystals showed a monatonic increase in fluorine-ion concentration with increasing CaF_2 in the melt. A correlation thus exists between the number of X centers in a FAP crystal and fluorine deficiency. (b) By growing crystals from a melt containing a deficiency of oxygen (achieved by using a deficiency of CaO), a correlation thus exists between the X-center concentration and an oxygen excess. This evidence, that the X center requires both fluorine-ion vacancies and excess oxygen, suggests that the X center is some kind of an oxygen-vacancy center. This is in agreement with the conclusion of Prener *et al.* concerning the nature of this center and its common occurrence in FAP. (c) By the addition of manganese (or certain other polyvalent metal ions) to the melt, Fig. 3 shows how the incorporation of increasing amounts of manganese in our crystals suppresses the X-center luminescence. This effect

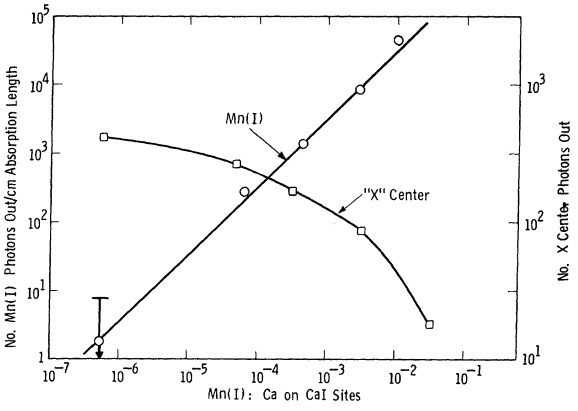

FIG. 3. Quantum yield of Mn(I) and X-center fluorescence versus concentration of Ca(I)-type Mn^{+2} determined from spin resonance. Number of photons are only relative.

is also shown by the magnitude of the optical absorption of the X center in crystals pulled from stoichiometric melts which decreases by at least two orders of magnitude as the manganese concentration in the melt is increased from a few ppm to 10%. The incorporation of manganese into FAP crystals thus somehow reduces the number of X centers. We believe this occurs by the formation of a complex of Mn and the X center and that the Mn(IIm) site is a complex of this sort.

VI. SPECTROSCOPIC PROPERTIES OF Mn^{+2} LOCATED ON A SIMPLE Ca(I) SITE

In all cases the assignment of excitation and fluorescence bands in our crystals to a particular type of manganese was done through an examination of the ESR data. By varying the growth conditions of the crystals, the relative numbers of different types of manganese could be varied greatly. For example, growing a crystal in a CaO-deficient melt completely suppresses the formation of the Mn(Im) and Mn(IIm) species. The 0.1%-Mn CaO-deficient crystal listed in Table I is an example of such a crystal. It contains only Mn(I) and Mn(II), mostly Mn(I). As we were unable to grow crystals containing only Mn(I), and free of Mn(II), or vice versa, the problem arose of differentiating between the optical properties of the two species.

The following experiment was performed to resolve this question. Two crystals were chosen that had widely different ratios of Mn(I) to Mn(II). Crystal A consisted of 10% Mn and $3\times CaF_2$ and crystal B had a 1% Mn stoichiometric. ESR results showed that the ratio of Mn(I) in crystal A to crystal B was 140:1, ±20%, whereas the ratio of Mn(II) in crystal A to crystal B was 1800:1, ±20%. Both crystals showed essentially identical optical properties, excitation, and fluorescence, so that one species was primarily responsible for the optical properties in both crystals. Samples identical in size, polish, and orientation were prepared from each crystal. The total fluorescent output of each crystal was then carefully measured while exciting into one of the weak Mn^{+2} absorption bands. The absorptions in the crystals were so weak that far less than 1% of the exciting light was absorbed in the crystals. Because of this the excitation was very uniform throughout the crystals and the fluorescent intensity was proportional to the number of absorbing centers per unit volume. The ratio of the fluorescent intensity of crystal A to crystal B was found to be 143:1, ±5%. The agreement of this ratio and the ratio of the number of Mn(I) ions in the two crystals and the disagreement with the ratio of the number of Mn(II) ions clearly rules out Mn(II) ions and proves that the Mn(I) ions are responsible for the observed excitation and fluorescent spectra.

The fluorescence envelope for Mn(I) ions at 300 °K is plotted in Fig. 4, at 1.8 °K in Fig. 7, and its excitation spectra at 1.8 °K in Fig. 5. The wavelength of the lines shown in the excitation data are summarized in Table II. An absorption measurement is shown in Fig. 6. The excitation data are a composite of the Mn(I) data obtained from many crystals. Since we were unable to grow crystals containing *only* Mn(I), every Mn(I)-type excitation spectrum measured contained some extra lines due to other types of Mn^{+2}. We have removed these lines in plotting Fig. 5 so that only the Mn(I) excitation peaks appear. It is possible, however, that a few spurious minor peaks due to other Mn^{+2} yet remain.

The Mn(I) optical absorption could be measured only in the highest concentration samples. The resolution of Fig. 6 is poor compared to Fig. 5 because of the high Mn concentration needed. The "axial" absorption spectrum measured for light propagating along the c axis is essentially identical to the "$E\perp C$" absorption spectrum measured with light propagating perpendicular to the c axis, indicating that the transition is of electric-dipole character. The absorption baseline of the "$E\parallel C$" and "$E\perp C$" spectra are higher than for the "axial" case because of linelike inclusions that formed inside this crystal along the direction of the c axis, which were less effective in scattering the "axial" light than the "$E\parallel C$" or "$E\perp C$" light.

The fluorescence envelope of Mn(I) is about 80%

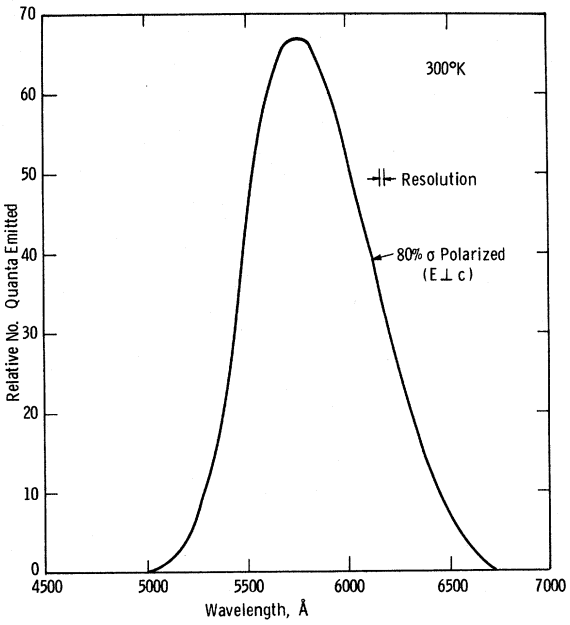

FIG. 4. Fluorescence emission spectrum of Mn(I) at 300 °K.

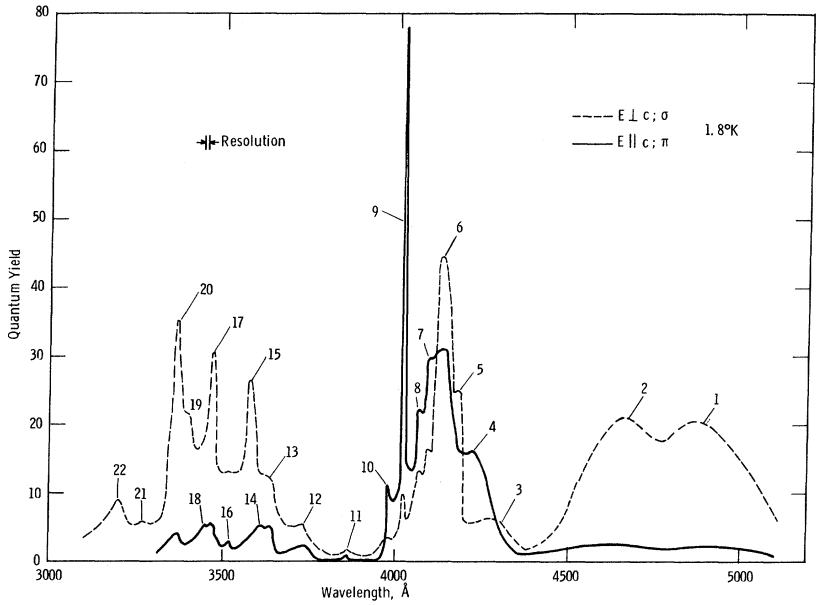

FIG. 5. Excitation spectra of Mn(I) fluorescence at 1.8 °K.

polarized $E \perp C(\sigma)$; both components have the same spectral distribution. Identical fluorescence envelopes were observed for samples containing as little as 0.01% manganese (relative to total calcium) and as much as 2%. The decay time of the fluorescence is 8 msec at 300 °K and below. All portions of the envelope have the same decay time and the spectra were found to be identical for all times following excitation, from 1 μsec of decay to 50 msec later. All of this suggests that we are seeing a simple single-ion fluorescence and that little interaction or pairing occurred between the ions in our crystals. The only interaction effect that we have observed is a broadening of the sharp peaks in the Mn(I) excitation spectra and a broadening of the lines of the ESR spectra for high manganese concentrations. The absorption strength and the fluorescence lifetime of Mn(I) are essentially temperature independent from 1.8 to 300 °K. No fine structure, such as a zero-phonon line, was found in the fluorescence envelope at low temperatures.

The excitation spectra shown on Fig. 5 are typical for a crystal containing only 0.02% manganese at 1.8 °K. Many of the sharp lines in the spectra

TABLE II. Excitation lines of Mn(I) at 1.8 °K.

Line No.	λ(Å)	Energy (cm^{-1})	Full width at half-maximum (cm^{-1})	Polarization
1	4870	20530	1250	σ
2	4610	21690	1150	σ
3	4285	23340	760	σ
4	4222	23690	<400	π
5	4180	23920	<170	σ
6	4132	24200	350	σ
7	4100	24390	<200	π
8	4070	24570	<200	a
9	4037	24770	60	π
10	3985	25090	<100	π
11	3865	25870	<100	a
12	3735	26770	290	a
13	3640	27470	<300	σ
14	3610	27700	<300	a
15	3580	27930	230	σ
16	3515	28450	<300	a
17	3470	28820	230	σ
18	3450	28990	<300	a
19	3400	29410	260	σ
20	3372	26660	260	σ
21	3260	30630	<700	σ
22	3200	31250	680	σ

[a]Not strongly polarized.

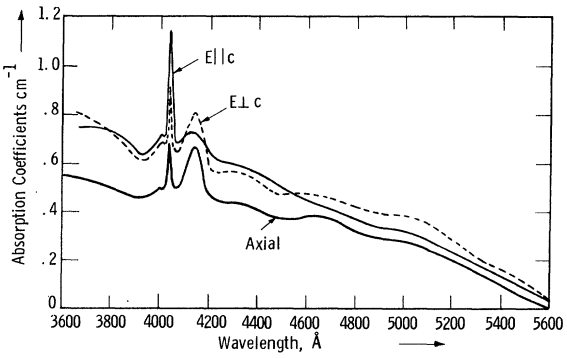

FIG. 6. Optical absorption at 4.3 °K of Mn(I).

broaden at higher temperatures and in crystals containing more manganese. Even in the worst case of a crystal at 300 °K containing 2% manganese, the excitation spectra are essentially identical, only broader, with many of the minor peaks being unresolvable. The existence of such detail in the excitation spectra tempts one to try to analyze it in detail. At first glance, the excitation spectra look quite similar to those observed by others for Mn^{+2} in a variety of hosts with octahedral sites for the Mn^{+2}. If the Ca(I)-type site were indeed cubic, line No. 8 would be termed a degenerate $^4A_{1g}$, $^4E_{1g}$ line, and line No. 1 a $^4T_{1g}$ line. The fluorescence would be assumed to come from the Stoke's shifted $^4T_1$ state to the $^6A_1$ ground state.

The Ca(I) site, however, is not a cubic site but has C_3 symmetry. It may be viewed as an octahedral site subjected to two very strong distortions. The principal distortion $T_2\mu$ is one in which the triangles of oxygen atoms above and below the Ca(I) site are twisted relative to one another. In the $T_1\mu$ distortion the center of mass of the six oxygens is displaced vertically away from the Ca(I) site. In FAP these distortions are sufficient to make a cubic approximation invalid.[13] Narita[13] has published the only calculation of the crystal field effects of the C_3 symmetry on the d^5 configuration of Mn^{+2}. Unfortunately, there is some error in his calculation as he finds, for instance, that the C_3 symmetry removes all degeneracies of the d^5 configuration. In fact, one can show that the C_3 point group cannot remove all of degeneracy of the d^5 configuration, but leaves the states belonging to complex-conjugate representations doubly degenerate due to time-reversal symmetry.[14] Thus, doubt exists in the validity of his results and we present no fit of our data to his calculations. We have presented the energy levels of Mn^{+2} in a site of C_3 symmetry in as great a detail as possible, so that if, in the future, such a calculation is performed, an accurate comparison with our data will be possible.

A calculation of the oscillator strength of Mn(I) was performed using the optical-absorption data and the EPR count for Mn(I) in the 10%-Mn stoichiometric crystal using the formula[15]

$$f=\frac{9n}{(n^2+2)^2}\left(\frac{mc^2}{\pi e^2}\right)\int \sigma\, d\nu\ ,$$

where σ is the absorption cross section. A value of $f=4\times10^{-7}$ was obtained. The predicted decay time was then calculated from the expression

$$1/\tau = 8\pi^2 \bar{\nu}^2 n^2 c\,(g_L/g_u)\int \sigma\, d\nu,$$

where g_L is the degeneracy of the ground state (assumed to be 6) and g_u is the degeneracy of the excited state (assumed to be 4). The calculated decay time is 17 ± 6 msec compared to 8 msec observed. The above expressions apply only to the case where the energy levels for absorption and fluorescence are identical. The Mn(I) energy levels experience a large Stoke's shift between absorption and fluorescence. In view of this, we consider the agreement between the two values of decay time to be reasonable.

VII. OPTICAL PROPERTIES OF Mn^{+2} LOCATED ON A SIMPLE Ca(II) SITE

The ESR results show that the ratio of Mn(II) to Mn(I) increases sharply at high-melt concentrations of manganese. The optical properties of Mn(II) were sought by choosing a crystal with as much Mn(II) as possible and looking for new absorptions and fluorescence. After a careful study of the two 10%-Mn crystals listed in Table I, we observed that these crystals do, indeed, exhibit such spectra which we now assign to Mn(II). The fluorescence envelope of Mn(II) at 1.8 °K is shown in Fig. 7, along with the 1.8 °K fluorescence envelope of Mn(I) obtained from the same crystal (10% Mn, $3\times CaF_2$). The Mn(I) fluorescence was excited by pumping into the 4037-Å excitation peak for Mn(I) (peak No. 9 in Fig. 5), whereas the Mn(II) fluorescence was excited by pumping into the 4009-Å excitation peak for Mn(II) (peak No. 4 on Fig. 8). By detecting the combined fluorescence of the crystal at 5200 Å, we were able to achieve sufficient rejection of the Mn(I) fluorescence to obtain the excitation spectrum of Mn(II) which is shown on Fig. 8. The quality of this

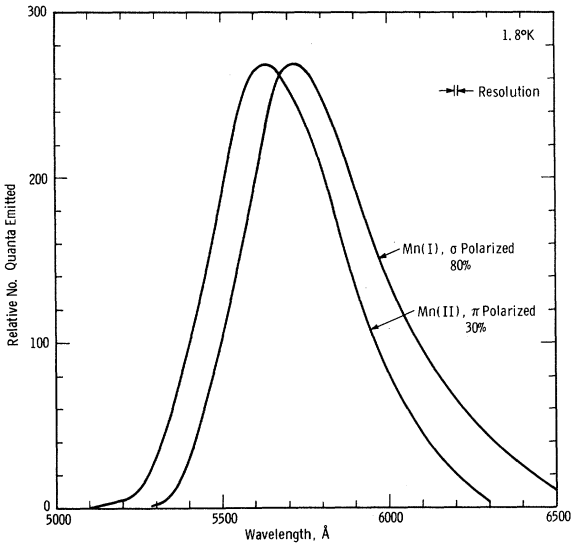

FIG. 7. Fluorescence emission spectrum of Mn(II) at 1.8 °K. The Mn(I) fluorescence emission is also plotted for comparison.

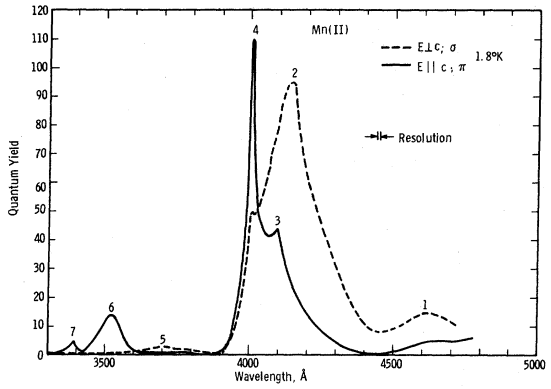

FIG. 8. Excitation spectra of Mn(II) at 1.8 °K.

excitation spectrum is poor relative to that we were able to achieve for Mn(I). One reason for this is that we were forced to obtain it in crystals containing high concentrations of manganese, which resulted in broadening of the energy levels. The other reason is that, by being forced to view only the small amount of Mn(II) fluorescence being emitted near 5200 Å, the signal-to-noise ratio during our excitation measurement required rather wide slits to be used in the excitation monochromator, resulting in a further loss of detail. The data of Fig. 8 are summarized in Table III. Although we were unable to measure the decay time of Mn(II), we were able to establish that it is equal to or greater than the decay time of Mn(I). Its oscillator strength is estimated to be approximately the same as the oscillator strength of Mn(I). The Mn(II) oscillator strength was estimated from comparing the relative areas under the Mn(I) and Mn(II) excitation spectra with the ESR values for the relative Mn(I) and Mn(II) concentrations, since optical-absorption data on Mn(II) could not be obtained in our crystals.

One can see from the fluorescence envelopes on Fig. 7 and the excitation spectra on Figs. 5 and 8 that Mn(I) and Mn(II) have fluorescence and excitation spectra that differ only very slightly. The major differences are the π fluorescence polarization of Mn(II) compared to the σ polarization of Mn(I), and the π excitation polarization of Mn(II) in the vicinity of 3500 Å compared to the σ polarization of the Mn(I) excitation peaks near 3500 Å.

In making the assignment of these spectra to Mn(II) we have had to rule out the possibility that they might, instead, be due to Mn at some other site, in particular Mn(I) pairs. The following arguments can be given against assigning these spectra to such pairs.

(i) Parodi[16] performed magnetic susceptibility measurements on a series of FAP powders containing Mn^{+2} concentration varying from 1 to 50% of the total calcium present. His results can be fitted with a model where manganese ions behave as a random mixture rather than one in which the manganese enters as pairs. One would therefore expect the concentration of pairs in FAP to vary as the square of the concentration of Mn(I) in the crystals. We find that the excitation strength, and therefore the optically determined concentration of the center that we have labeled Mn(II), is proportional to the ESR-determined concentration of Mn(II) and not to the square of the Mn(I) concentration. For example, the ratio of the number of randomly produced pairs in the 10%-Mn $3\times CaF_2$ crystal to the 1%-Mn stock crystal is calculated to be about 20 000:1, whereas the Mn(II) ratio measured by ESR is 1800:1, and the Mn(II) ratio measured by fluorescence is about 2000:1. Clearly, the fluorescent intensities are consistent with the Mn(II) center but cannot be reconciled with the 20 000:1 ratio expected of pairs.

(ii) If the optical spectra labeled Mn(II) are due to pairs, why have we failed to observe the excitation and fluorescence spectra of Mn(II), especially in the 10% crystals where ESR measurements indicate that large numbers of Mn(II) ions are present? We would only fail to see the Mn(II) spectra if (a) the excitation and fluorescence spectra were essentially identical in all respects to the Mn(I) spectra so that they were masked by the Mn(I) spectra, or (b) its absorption strength was a factor of almost 100 lower than the absorption strength of the Mn(I) ions. Possibility (a) is unlikely because the C_3 symmetry of the Ca(I) site and the C_{1h} symmetry of the Ca(II) site are quite different and therefore should not produce identical energy levels for Mn^{+2}. Possibility (b) is unlikely because it would predict a decay time in the order of 1 sec for Mn(II). Such a long decay time has never been observed for Mn^{+2} situated in any host, even in sites of high symmetry.

(iii) The existence of pairs has been looked for by ESR techniques. In particular, exchange-coupled pairs like those seen by McClure[17] were searched for at 1.8 and 77 °K and not seen.

TABLE III. Excitation lines of Mn(II) at 1.8 °K.

Line No.	λ(Å)	Energy (cm^{-1})	Full width at half-maximum (cm^{-1})	Polarization
1	4630	21 600	>1200	σ
2	4140	24 150	1050	σ
3	4090	24 450	<150	π
4	4009	24 940	< 80	π
5	3700	27 030	...	σ
6	3520	28 410	650	π
7	3385	29 540	350	π

In spite of these arguments, the assignment of these optical properties to Mn(II) is less certain than the other assignments reported here.

VIII. SPECTROSCOPIC PROPERTIES OF Mn^{+2} LOCATED ON Ca(II) MODIFIED SITE

Manganese-doped crystals pulled from stoichiometric melts invariably contain some Mn(II*m*). As can be seen in Table I, the concentration of Mn(II*m*) centers shows a saturation effect, with the largest percentage of manganese entering into these sites as low manganese concentrations and the lowest percentage at high manganese concentrations. For a given total manganese concentration, the concentration of Mn(II*m*) centers can be reduced by as much as an order of magnitude by using excess CaF_2 in the melt. The reduction is even more marked in crystals pulled from calcium-oxide deficient melts where the formation of Mn(II*m*) centers is completely suppressed. The optimum conditions for growing crystals containing large amounts of Mn(II*m*) are therefore identical to the conditions for growing crystals containing large amounts of oxygen-fluorine-ion vacancy-defect complexes such as the *X* center.

The 77 °K fluorescence emission envelope of this center in the 1% stoichiometric crystal is shown in Fig. 9. Its emission is completely thermally quenched by 300 °K so that excitation spectra taken at 300 °K show no evidence of its presence. Its emission envelope is twice as broad as the emission envelope of Mn(I) and its peak position is at a longer wavelength. It is σ polarized approximately 65% ($E \perp C$). Its decay time at 77 °K is approximately 4 mscc.

The Mn(II*m*) excitation spectra are shown in Figs. 10 and 11 at 1.8 and 77 °K, respectively. Some interesting features are apparent in these spectra. The lowest-energy excitation peak numbered 5 is strongly σ polarized as is the fluorescence emission envelope. This suggests that it is the energy level from which the fluorescence transition occurs, following a large Stoke's shift of over 2000 Å. Such a large Stoke's shift implies a great deal of relaxation of the environment of the Mn(II*m*) site as does the thermal quenching of the fluorescence. The Mn(II*m*) site in which a manganese ion is substituted for a Ca(II) atom adjacent to an oxygen-fluorine-ion vacancy-defect complex might be expected to provide a "soft" environment where such a large relaxation could occur due to the presence of the vacancy.

Another interesting feature of the excitation spectra is the temperature-dependent behavior of the lines numbered 3 and 4. The excitation spectra for the Mn(I) or Mn(II) center show little change with temperature between 1.8 and 77 °K, but lines 3 and 4, which are present at 77 °K, all disappear upon cooling to 1.8 °K. The energies of these lines are listed in Table IV. From the constancy of their spacing of 560 cm^{-1}, lines 3 and 4 appear to be satellites of lines 1 and 2. A simple model for explaining the thermally activated appearance of satellite absorptions 3 and 4 at lower energies than lines 1 and 2 is shown in Fig. 12(a). The lines 3 and 4 are assumed to be absorptions to the same pair of upper levels as 1 and 2 but originating from a state 560 cm^{-1} above the ground state. A difficulty with this model is that since the population of the thermally excited state would be only $\sim 10^{-4}$ at 77 °K one would

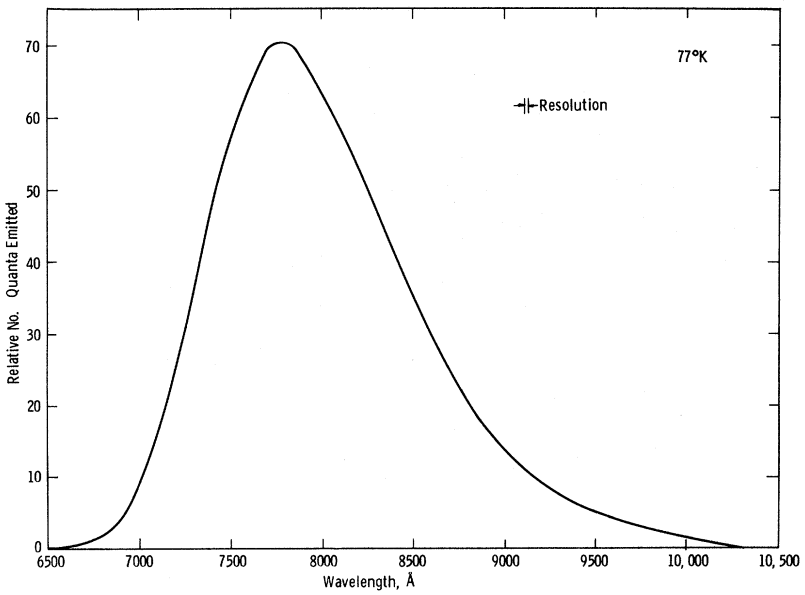

FIG. 9. Fluorescence emission spectrum of Mn(II*m*) at 77 °K.

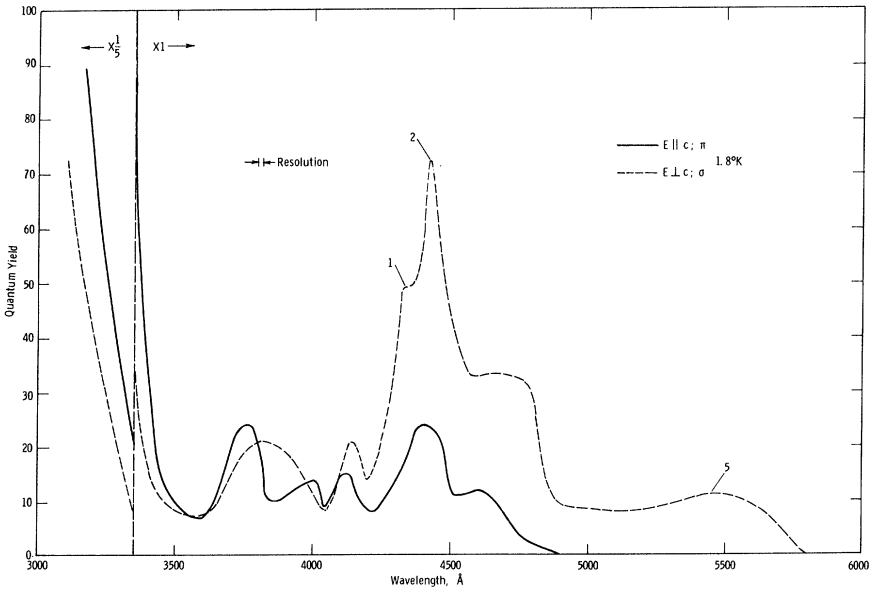

FIG. 10. Excitation spectra of Mn(II*m*) at 1.8 °K.

require an absorption strength for transitions originating in the thermally populated state to be $\sim 10^4$ higher than for transitions originating in the ground state in order to account for the strength of lines 3 and 4 relative to 1 and 2 at 77 °K. Such a large increase in absorption is unrealistic.

A more reasonable model is shown in Fig. 12(b), where absorptions 3 and 4 are lower in energy than 1 and 2 because the excited states have been lowered in energy by a thermal-activated process. A likely process is suggested in Fig. 12(c). Here the Mn(II*m*) is pictured as a manganese ion substituting for a Ca(II) ion, with a fluorine-ion vacancy and a substitutional oxygen located adjacently, although a more complicated oxygen-fluorine-ion vacancy-defect complex could have been chosen with equal justification. The thermally excited process would be one in which the vacancy and oxygen interchange positions, one configuration being stable at very low temperatures and another at higher temperatures. This alteration would probably have less effect on the ground state of the Mn complex than on the excited state which involves more spatially extended wave functions. The observed 560-cm^{-1} shift would therefore be related to the magnitude of the excited-state shift and not the thermal activation energy of

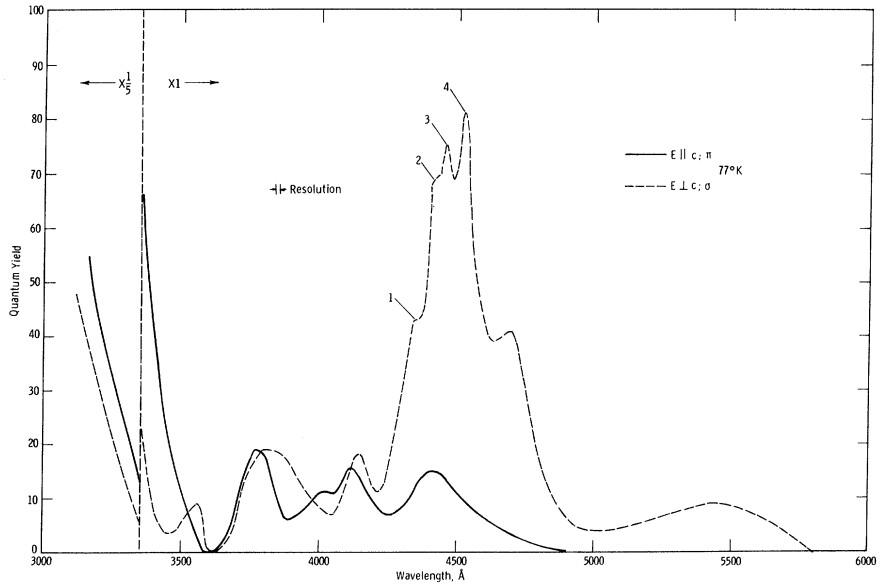

FIG. 11. Excitation spectra of Mn(II*m*) at 77 °K.

TABLE IV. Excitation lines of Mn(II*m*) at 77 °K. Only those lines discussed in the text are listed.

Line No.	λ(Å)	Energy (cm^{-1})	Full width at half-maximum (cm^{-1})	Polarization
1	4350	22 990	~200	σ
2	4415	22 650	~200	σ
3	4458	22 430	~200	σ
4	4527	22 090	~200	σ
5	5450	18 350	>1400	σ

the process. This model is, unfortunately, also of doubtful validity. A movement between sites of an oxygen ion would alter the surroundings of the Mn^{+2} ion which should cause a change in the ESR spectrum. Very careful measurements of the ESR spectra at 4.2 and at 22 °K of the Mn(II*m*) site in the 1% stoichiometric crystal showed no change with temperature. We therefore must leave the explanation of this thermal effect open at the present time.

A final interesting feature of the Mn(II*m*) excitation spectra is the anomalously strong excitation below 3500 Å, where the strength becomes orders of magnitude larger than at wavelengths above 3500 Å. No comparable excitations occur in the spectra of Mn(I) or Mn(II). We attribute this excitation to energy absorbed by the oxygen-fluorine-ion vacancy part of the Mn(II*m*) complex and transferred to the manganese ion. These complexes have strong optical absorption below 3500 Å in undoped crystals,[11] and it is reasonable to assume that their absorptions would not be altered greatly by substituting a manganese ion for one of the neighboring Ca(II) ions, and thus they could account for the strong absorptions observed in the excitation spectra.

IX. OPTICAL PROPERTIES OF Mn^{+2} LOCATED ON Ca(I) MODIFIED AND OTHER UNIDENTIFIED SITES

In addition to the optical spectra that we have assigned to Mn^{+2} located on particular lattice sites, we have observed "extra" excitation peaks and fluorescences, especially in crystals with high Mn concentrations. It is reasonably clear that these are due to manganese since they are absent in undoped crystals and exhibit long decay times, but to date we have been unable to correlate any of these phenomena with ESR data and arrive at a firm assignment of the types of sites responsible. This is due primarily to the difficulty of observing different species of Mn^{+2} by ESR in these crystals containing large (1% and higher) concentrations of manganese. The emissions that we have observed from these unidentified sites lie in the infrared with broad peaks between 7000 and 7500 Å; they are thermally quenched by 300 °K. Their corresponding excitation spectra show no sharp excitation structure but consist of a series of broad bands. They also show anomalously strong absorptions below 3500 Å as does the Ca(II) modified type of Mn^{+2}. This suggests that the centers responsible might be due to Mn^{+2} adjacent to various combinations of oxygen-vacancy complexes, different from those involved in the Ca(II*m*) centers.

We have not been able to observe the optical properties of Mn^{+2} located on the Ca(I) modified site. The ESR spectra show the Ca(I*m*) site to be a slight distortion from the simple Ca(I) site. Any modification in the optical properties of the Ca(I) site due to this distortion would probably also be slight. Since we were unable to resolve excitation peaks located less than 30 cm^{-1} apart we believe that the Mn(I*m*) excitation peaks are shifted less than 30 cm^{-} from the Mn(I) peaks and they cannot be observed by us with our limited resolution. In the same way the Mn(I*m*) fluorescence is hidden by the Mn(I) fluorescence.

X. SUMMARY AND CONCLUSIONS

We have observed and identified the optical properties of divalent manganese situated on the Ca(I) site, the Ca(II) site, and a modified Ca(II) site. Undoped crystals or crystals containing low manganese concentrations pulled from stoichiometric melts show strong absorption and fluorescence due to *X* centers. The numbers of these *X* centers present in the crystal increases as growth conditions are made favorable for producing fluorine vacancies and substitutional oxygen impurities. The number of *X* centers decreases as the manganese concentration in the crystals is increased. The disappearance of the *X* center is matched by the growth of the Mn(II*m*) center. We conclude that the *X* center is due to an oxygen-vacancy complex and that manganese situating nearby at a Ca(II) site annihilates the *X* center in forming the Mn(II*m*) center.

In most of the crystals studied, the Mn(I) center clearly dominates the optical excitation, absorption, and fluorescence emission observed. The optical properties of the Mn(II) center are most easily observed in crystals containing 1% or more manganese

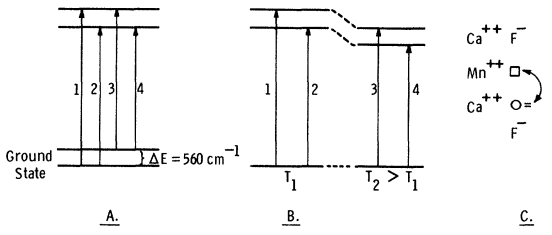

FIG. 12. Models for explaining the thermal changes in the Mn(II*m*) excitation spectra.

since its incorporation into the crystals increases strongly with manganese concentration. The Mn(II*m*) center dominates the optical excitation and fluorescence in crystals containing low concentrations of manganese pulled from stoichiometric melts. The Mn(II*m*) fluorescence is thermally quenched by 300 °K. The Mn(I*m*) center, detected by ESR, was not observed in excitation or fluorescence, probably because of the insignificant deviations of its optical properties from those of the Mn(I) center. Additional excitation and fluorescence spectra were observed in some crystals that have not been assigned to any specific model. Because of the similarity of their optical properties to the optical properties of the Mn(II*m*) center, we feel that these centers are due to divalent manganese located adjacent to various oxygen-vacancy complexes, but differing from the complex that forms the Mn(II*m*) center.

ACKNOWLEDGMENTS

We would like to thank Dr. W. Partlow for measuring the decay time of the *X* center. W. Kramer grew most of the crystals described in this work, and P. Handke gave technical assistance.

[1]K. H. Butler and C. W. Jerome, J. Electrochem. Soc. 97, 265 (1950).

[2]P. D. Johnson, J. Electrochem. Soc. 108, 159 (1961).

[3]P. H. Kasai, J. Phys. Chem. 66, 674 (1962).

[4]P. D. Johnson, Bull. Am. Phys. Soc. 6, 30 (1961).

[5]P. D. Johnson, in *Luminescence of Organic and Inorganic Materials*, edited by H. P. Kallmann and G. M. Spruch (Wiley, New York, 1962), p. 563.

[6]R. Mazelsky, R. C. Ohlmann, and K. B. Steinbruegge, J. Electrochem. Soc. 115, 68 (1968).

[7]R. Mazelsky, R. H. Hopkins, and W. E. Kramer, J. Crystal Growth 34, 260 (1968).

[8]Types KM-2901 and KM-2866 available from Fairchild-Dumont Labs., Clifton, N. J.

[9]J. Murphy and F. M. Ryan, Bull. Am. Phys. Soc. 13, 415 (1968).

[10]Y. Ohkubo, J. Phys. Soc. Japan 18, 916 (1963).

[11]Y. Ohkubo and H. Mizuno, Proceedings of the International Conference on Luminescence, Budapest, 1966 (unpublished), p. 6.

[12]J. S. Prener, W. W. Piper, and R. M. Chrenko, J. Phys. Chem. Solids 30, 1465 (1969).

[13]K. Narita, J. Phys. Soc. Japan 16, 99 (1961).

[14]J. L. Prather, Natl. Bur. Std. (U. S.) Monograph 19, 52 (1961).

[15]W. B. Fowler and D. L. Dexter, Phys. Rev. 128, 2154 (1962).

[16]J. A. Parodi, J. Electrochem. Soc. 116, 1550 (1969).

[17]D. S. McClure, J. Chem. Phys. 39, 2850 (1963).